European Radiology (2019) 29:6300–6308
https://doi.org/10.1007/s00330-019-06251-3

INTERVENTIONAL

Single-needle electroporation and interstitial electrochemotherapy: in vivo safety and efficacy evaluation of a new system

Federico Pedersoli[1] · Andreas Ritter[1,2] · Markus Zimmermann[1] · Maximilian Schulze-Hagen[1] · Martin Liebl[1] · Ebba Dethlefsen[1] · Saskia von Stillfried[3] · Joachim Pfeffer[1] · Christiane K. Kuhl[1] · Philipp Bruners[1] · Peter Isfort[1]

Received: 26 February 2019 / Revised: 12 April 2019 / Accepted: 24 April 2019 / Published online: 17 May 2019

Abstract

Objectives We conducted an in vivo trial to investigate the safety and efficacy of a newly developed system for the application of a combined therapy consisting of irreversible electroporation (IRE) and electrochemotherapy (IRECT) in the liver. The system is conceived as a single-needle multitined applicator with expandable electrodes that allow interstitial injection of fluids, e.g., chemotherapy.

Methods Experiments were conducted in ten domestic pigs. The applicator was placed in different liver lobes under CT guidance. In one lobe, the applicator was used for conventional IRE (1500 V, 120 pulses, pulse length 100 μs). In the other lobe, the same procedure was performed preceded by the injection of a doxorubicin mixture through the expandable electrodes (IRECT). Contrast-enhanced CT and MRI were performed on days 1, 3, and 7 after the procedure. Accordingly, three animals were sacrificed on days 1, 3, and 7 after the imaging and ablation volumes were evaluated histopathologically. Related *t* test was used to compare the groups.

Results Technical success was achieved in 9/10 experiments. One animal deceased during the intervention because of ventricular fibrillation. Follow-up CT 1 and 3 days after intervention showed a significant ($p < 0.05$) difference in the ablation volumes of IRECT vs IRE, respectively, of 4.47 ± 1.78 ml vs 2.51 ± 0.93 ml and of 3.39 ± 1.05 vs 1.53 ± 0.78 ml.

Conclusions IRECT using the newly developed system proved to be effective and provided significantly larger ablation volumes compared with IRE alone. However, ECG triggering is a necessary prerequisite to allow a safe application of the system.

Key Points

- *Working on the geometry of the IRE applicator in terms of expandable electrodes may overcome the current limitations of IRE resulting from the placement of multiple electrodes.*
- *Efficacy of IRE ablations can be enhanced by the interstitial application of chemotherapy in the periphery of ablation areas.*

Keywords Electroporation · Electrochemotherapy · Electrodes

Abbreviations

ECT	Electrochemotherapy
IRE	Irreversible electroporation
IRECT	Irreversible electroporation and electrochemotherapy

Philipp Bruners and Peter Isfort contributed equally to this work.

✉ Federico Pedersoli
fpedersoli@ukaachen.de

[1] Department of Diagnostic and Interventional Radiology, RWTH University Hospital Aachen, Pauwelsstrasse 30, 52074 Aachen, Germany

[2] Helmholtz-Institute for Biomedical Engineering, RWTH Aachen University, Pauwelsstraße 20, 52074 Aachen, Germany

[3] Pathology Institute, RWTH University Hospital Aachen, Pauwelsstrasse 30, 52074 Aachen, Germany

Introduction

Electroporation is based on the application of a short, high-intensity, pulsed electric field in tissues which increases the cellular permeability to water, ionic, and large molecules by means of formation of nanometer-sized pores in the cellular membrane [1]. Depending on the characteristics of the applied electric field, the state of increased permeability can be reversible, lasting minutes after its application, or irreversible [2].

In biotechnology, reversible electroporation has been used for years for cell fusion or intracellular gene delivery and it is

gaining an increasing attention in medicine in terms of electrochemotherapy (ECT). ECT exploits the reversible state of increased membrane permeability to achieve a higher intracellular uptake of chemotherapeutic agents. So far, ECT has been proven to be an effective and safe technique for the palliative treatment of superficial skin and subcutaneous malignancies [3], whereas its role in the treatment of liver [4], breast [5], and head-neck tumors [6] is still under debate.

If the intensity of the electric field exceeds a certain threshold, cells cannot withstand the electrolytic impairment and undergo cell death by means of apoptosis, a mechanism that is called irreversible electroporation (IRE) [7]. IRE is a comparably new technique for the image-guided ablation of tumors of the liver [8], pancreas [9], kidney, prostate, and bone [10]. The main advantage of IRE compared with thermal ablative therapies, like radiofrequency or cryoablation, is the non-thermal mode of action. The heat sink- or cold sink effect does not play a role in IRE because of its non-thermal properties [11]. IRE is currently performed in a clinical setting with the NanoKnife System (AngioDynamics, Inc.). With this system, multiple needle electrodes are placed in and around the tumor and then activated sequentially in order to achieve a sufficient strength of the electric field (> 1000 V/cm) in the target area. However, with increasing distance from the IRE electrodes, the field strength decreases and the electroporation effects become reversible, resulting in the survival of cells. Hence, we postulate that the local application of a chemotherapeutic drug in this area will lead to an increase in the volume of ablation, resulting in a combination therapy of IRE and ECT (IRECT).

Therefore, the primary aim of our study was to evaluate the efficacy and safety of a custom-designed single-needle, multitined, expandable applicator for this local combination treatment in vivo, which was conceived, developed, and produced in our department [12]. The additional goal is to compare the additional effect given by the interstitial application of chemotherapy through the expandable electrodes with solely IRE ablations.

Materials and methods

IRE/ECT prototype

The custom-designed, handcrafted applicator prototype was conceived as a single needle-shaped applicator that features four hollow, expandable electrodes, which can be used for both injection of fluids in the liver parenchyma and for the application of high-voltage electric pulses (Fig. 1). The central electrode is charged positively and the four expandable electrodes are charged negatively. The central electrode has a diameter of 3.2 mm (ca. 8 gauge) and the expandable electrodes of 0.6 mm (ca. 22 gauge). The distance between the central electrode and the expandable electrodes with the opened applicator measures 12 mm and the active tips of the central electrode and the expandable electrodes measures 9.8 mm. According to our computer simulations, the application of the electrical field through the electrode produces a core of irreversibly electroporated cells surrounded by a "penumbra" of cells in a reversible state of electroporation [13], possibly allowing a higher uptake of cytotoxic substances (Fig. 2).

Animal experiments

After approval by the animal care authorities, experiments were conducted in ten female domestic pigs with a mean weight of 80 kg. All experiments were performed under general anesthesia after orotracheal intubation and mechanical ventilation under continuous monitoring of blood oxygenation level and heart rate. Blood test with full blood count, liver function test (transaminase, bilirubin, albumin), and CRP were obtained before the intervention and before each imaging follow-up session.

After animals were fixed on the CT table in supine position, a non-enhanced CT (Siemens Somatom Definition Flash; Siemens Healthineers) in end-expiratory breath-hold was performed to plan the placement of the applicator prototype. In order to achieve deep muscle relaxation, 4 mg of Pancuronium (Inresa Arzneimittel GmbH) was administered intravenously via a peripheral line placed in an ear vein. Then, the applicator prototype was placed sequentially in two distinct positions of the liver (separate liver lobes) under CT guidance. Thereafter, the applicator prototype was expanded and another CT was performed to confirm the correct position of the applicator in the central part of the liver lobe. Then, the electrodes were powered simultaneously by a high-voltage pulse generator (ECM® 630 Electroporation System, BTX Harvard Apparatus). In one position, the applicator was used for IRE using standard settings (field strength up to 1500 V/cm, 30 × 4 pulses, pulse length 100 μs). In the other position, IRECT was applied consisting of the same IRE procedure but preceded by the injection of a solution consisting of 50 mg doxorubicin (Pfizer Inc.) dissolved in 4.5-ml 0.9% saline solution and 1.5-ml contrast medium (Ultravist 370, Bayer AG) through the four expandable electrodes. The location of IRECT vs IRE in the left or right liver lobe was randomized.

Multiphase CT (non-enhanced, arterial and portal venous phase) and MRI (sequences: T2w-TSE, T2w-SPIR, DWI, T1 dynamic, and T1 GRE after intravenous administration of 0.1 mmol/kg gadoxetic acid) studies were performed to evaluate the ablation volumes after the intervention. Afterwards, animals were transferred to the animal research department to wake up from anesthesia.

Technical success of the intervention was defined as the formation of a new ablation in the absence of major adverse effects. In CT and MRI, ablations were defined as newly established non-contrast-enhancing areas of treatment effect

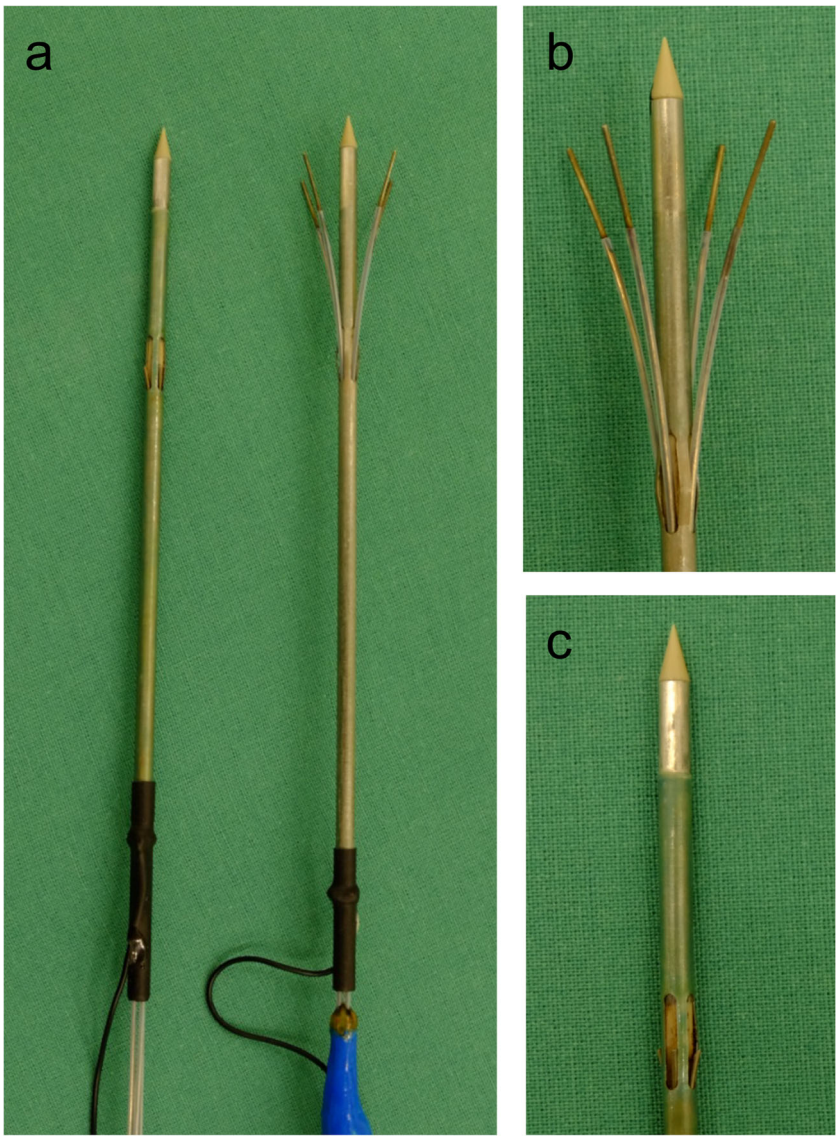

Fig. 1 Applicator prototype (**a**), and the tip of the applicator prototype in opened (**b**) and closed (**c**) positions

surrounding the former applicator position in follow-up 1 day after the intervention. Effectiveness of ablations on imaging was then evaluated during follow-up and correlated to pathological analysis.

Follow-up imaging

Follow-up imaging was performed with contrast-enhanced CT and MRI using the same parameters as in the post-interventional imaging. All animals underwent follow-up imaging on day 1 after the experiment. Thereafter, three animals were sacrificed (acute group). On day 3 after the experiment, the remaining six animals received follow-up imaging. Thereafter, another three animals were sacrificed (subacute group). On day 7 after the experiment, the remaining three animals were sacrificed after follow-up imaging (chronic group).

Imaging volume assessment of the area of treatment effect was performed with ROI segmentation (Multi-Modality Tumor Tracking application, IntelliSpace Portal, Philips) based on CT data in portal venous contrast phase.

Pathological evaluation

Livers were harvested and fixed in formalin. For pathological workup, livers were sliced in 5-mm-thick slices and analyzed macroscopically. All slices were documented photographically; a ruler for calibration purpose was placed nearby. The volume of the area of treatment effect was calculated multiplying the ablative areas with the slice thickness and the number of slices. Representative slices were dehydrated, paraffinized, cut into 4-μm cuts, and mounted on microscope slides (Langenbrinck) for staining on an H&E autostainer.

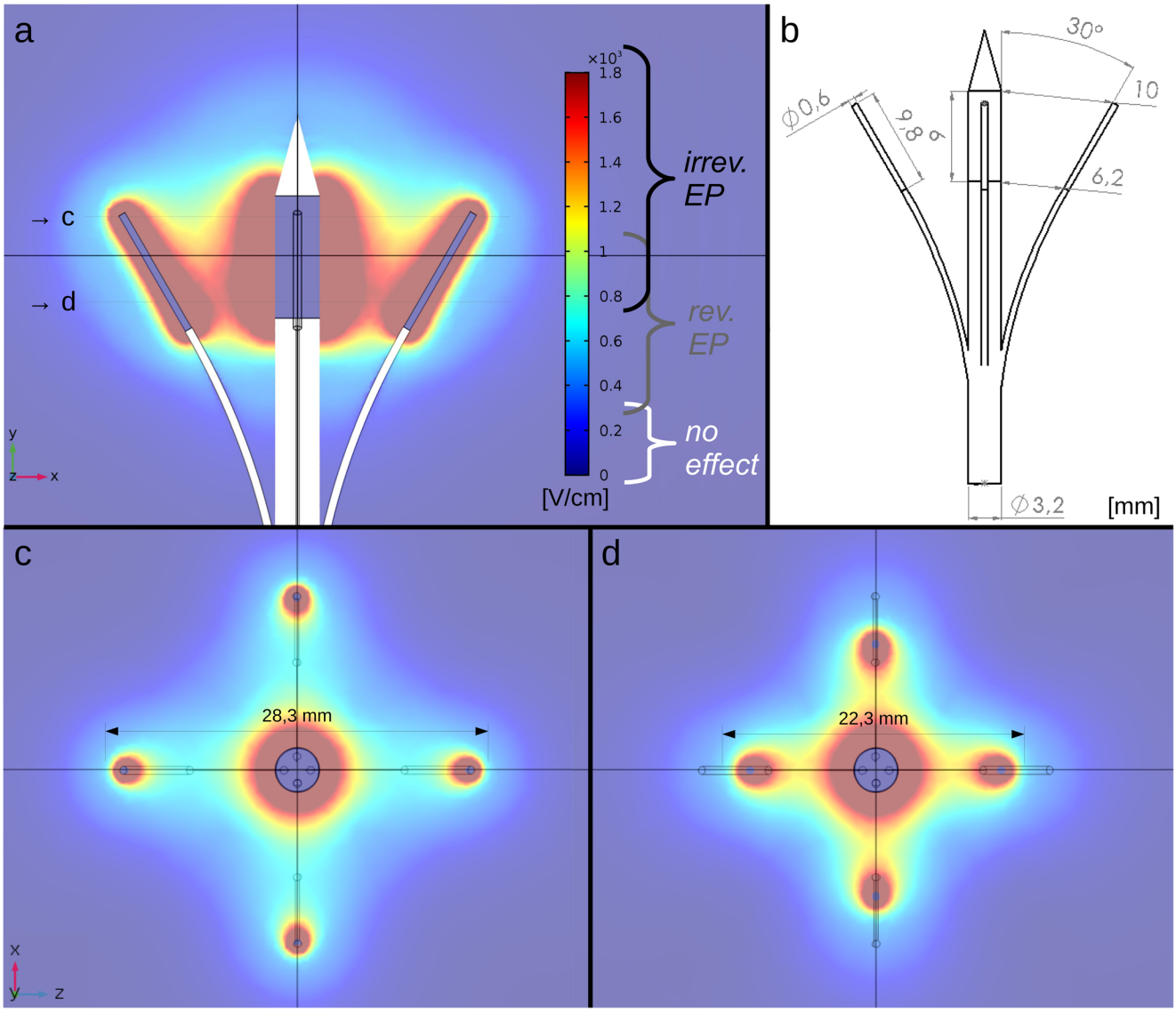

Fig. 2 Sectional plane of the simulated electrical field distribution for an applied voltage of $U = 1.5$ kV. Red area: $E \geq 1.3$ kV/cm; tissue in this area will be irreversibly electroporated (IRE). Dark-blue to light-blue area: $E \leq 0.35$ kV/cm; tissue in this area will not be harmed through electroporation. Area in between: reversible electroporation, target area for chemotherapeutic drugs (ECT). Sagittal section of the simulated electrical field (**a**). Sagittal section of the design of the tips of the applicator prototype (**b**). Axial sections of the simulated electrical field (**c**, **d**)

Necrotic areas in proximity of the placement of the applicator were considered as ablation zones.

Statistical analysis

SPSS (IBM) was used for statistical analysis. Average and standard deviation was calculated for all volumetric data derived from CT and macroscopical pathological analyses. Related *t* test was used to compare the groups. $P < 0.05$ was considered statistically significant. According to the structure of follow-up, volume data based on CT were available for 9 animals 1 day after the intervention, 6 animals 3 days after the intervention, and 3 animals 7 days after the intervention. Pathologic examination was possible on 3 animals 1 day, 3 days, and 7 days after the intervention.

Results

Technical success was achieved in 9 out of 10 animals. One swine developed ventricular fibrillation during the intervention after the first application of IRE and deceased despite multiple resuscitation attempts. Besides that, no major or minor complications were observed in both groups. After the approval of the animal care authorities, it was possible to conduct the intervention with a substitute animal in order to

have a homogeneous sample size of groups for statistical analysis. The intervention was subsequently successfully performed. The correct opened position of the applicator with the complete expansion of the electrodes and the achievement of the precise angle between the central electrode and the expandable electrodes was feasible in each animal.

Blood test did not show any alterations in blood count, transaminases, or CRP at any point of follow-up.

All ablations were detectable in CT, MRI, and pathological analysis.

Imaging

In CT, the area of treatment effect appeared as hypodense areas demarcating with sharp margins from the healthy liver parenchyma showing a perilesional enhancement in the arterial phase. On MRI, both areas of treatment effect exhibited a typical signal pattern with moderate hyperintensity on T2-weighted imaging and a lack of enhancement of the treated area and peripheral rim enhancement in T1-weighted imaging after administration of gadoxetic acid (Fig. 3).

Pathological analysis

In gross pathologic examination (Fig. 4), the treated zones in the liver specimens appeared red-brown and darker than the surrounding untreated liver parenchyma. The shape of the areas of treatment effect in the IRE group reflected precisely the geometry of the applicator, whereas ablations in the IRECT group were more irregularly defined (Fig. 4). In histological workup, ablated zone showed a preserved structure of the liver tissue, with intact vessel and bile duct walls, as well as preserved acinar architecture of the liver parenchyma with broad fibrous septae. Within the treatment zone, a uniformly eosinophilic center corresponded to the white coagulation necrosis on macroscopic evaluation. The nuclei within the treated zone were pyknotic. The vascular and bile duct walls within the ablation zones appeared macroscopically intact in both groups. Areas of central white coagulation necrosis measuring up to 2 mm were noted immediately surrounding the electrode insertion canal. A hemorrhagic rim in the periphery of the necrotic zone was seen mainly in the acute phase of follow-up in both groups and was progressively substituted by a fibrotic reaction with hypertrophy of biliary ducts. No qualitative differences between the two groups were observed.

Volumetry

Based on CT data, average ablation volumes after 1 day measured 2.51 ± 0.93 ml in the IRE group compared with 4.8 ± 1.78 ml for IRECT ($p = 0.003$); after 3 days 1.53 ± 0.78 ml for IRE vs 3.39 ± 1.05 ml for IRECT ($p = 0.005$); and after 7 days

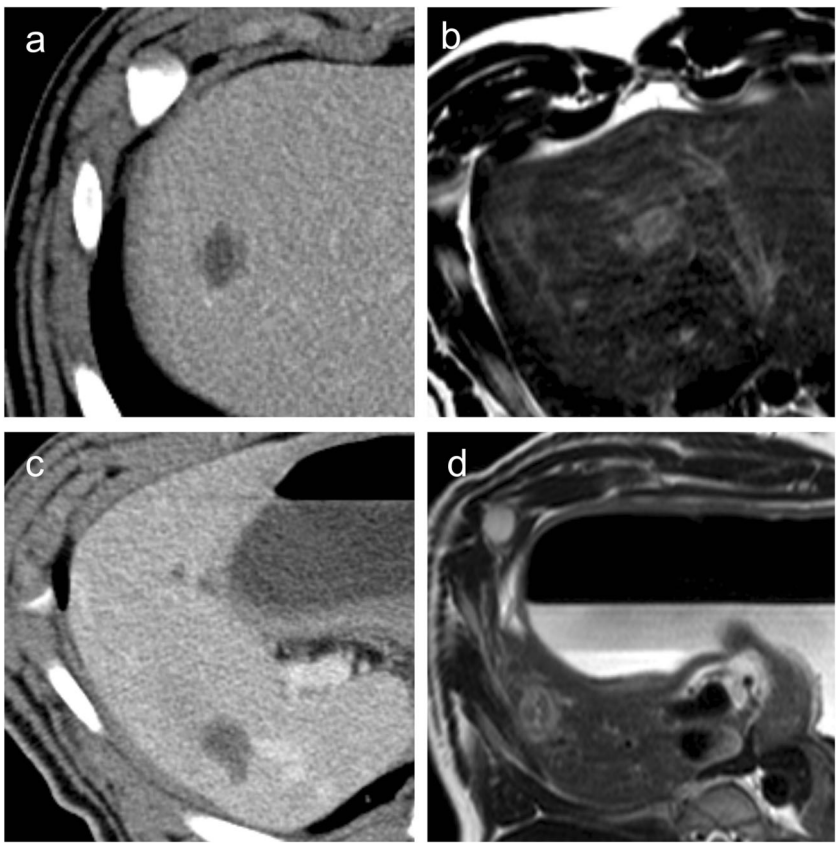

Fig. 3 Follow-up 1 day after the intervention. IRE ablation in CT in venous contrast phase (**a**) and in T2-MRI (**b**). IRECT ablation in CT in venous contrast phase (**c**) and in T2-MRI (**d**)

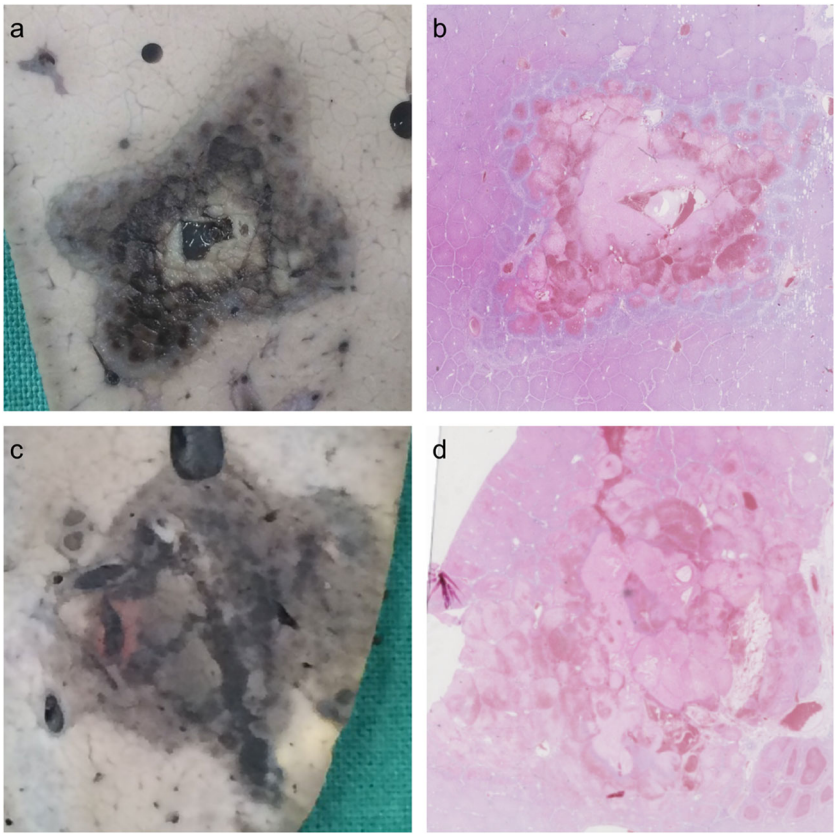

Fig. 4 Ablation of the IRE group 1 day after the intervention: macroscopical analysis after formalin staining (**a**), histopathological analysis of ablations after hematoxylin and eosin staining (**b**). Ablation of the IRECT group 1 day after the intervention: macroscopical analysis after formalin staining (**c**), histopathological analysis of ablations after hematoxylin and eosin staining (**d**)

0.69 ± 0.49 ml for IRE vs 2.28 ± 1.08 ml for IRECT ($p = 0.2$) (Fig. 5). Average axial (perpendicular to the central electrode) and sagittal diameter (parallel to the central electrode) of the ablation areas after 1 day based on CT measured respectively 1.6 ± 0.3 cm and 1.1 ± 0.3 cm for IRE vs 2.1 ± 0.5 cm and 1.4 ± 0.3 cm for IRECT; after 3 days 1.4 ± 0.2 cm and 1.2 ± 0.2 cm for IRE and 2.0 ± 0.5 cm and 1.3 ± 0.3 cm for IRECT; and after 7 days 0.9 ± 0.4 cm and 0.8 ± 0.2 cm for IRE vs 1.8 ± 0.8 cm and 1.2 ± 0.2 cm for IRECT.

In gross pathologic examination, average ablation volumes after 1 day measured 3.15 ± 1.53 ml for IRE vs 5.66 ± 4.30 ml for IRECT ($p = 0.2$); after 3 days 2.46 ± 0.87 ml for IRE vs 4.47 ± 1.71 ml for IRECT ($p = 0.3$); and after 7 days 1.56 ± 1.1 ml for IRE vs 3.49 ± 3.36 ml for IRECT ($p = 0.2$) (Fig. 5).

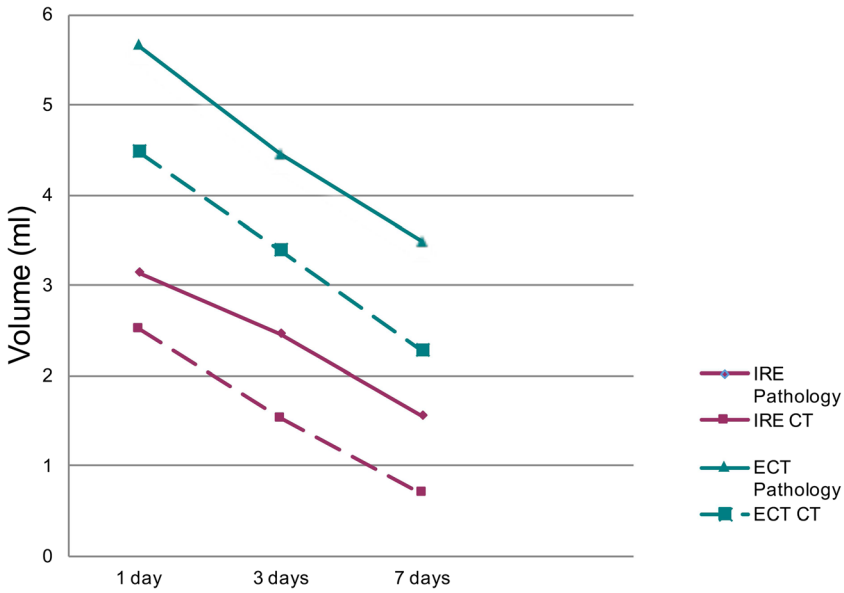

Fig. 5 Ablations volumes during follow-up

Average axial and sagittal diameter of ablations based on histopathological analysis data measured respectively after 1 day 1.9 ± 0.3 cm and 1.6 ± 0.1 cm for IRE vs 2.4 ± 0.4 cm and 1.7 ± 0.5 cm for IRECT; after 3 days 1.9 ± 0.3 cm and 1.4 ± 0.2 cm for IRE vs 6 ± 0.8 cm and1.4 ± 0.4 cm for IRECT; and after 7 days 1.6 ± 0.4 cm for IRE vs 2.2 ± 0.6 cm and 1.1 ± 0.5 cm for IRECT.

In CT imaging, the acute, subacute, and chronic group mean ablation volumes of IRECT were respectively 78% (1 day), 122% (3 days), and 228% (7 days) larger than in the respective IRE groups. In pathological evaluation, mean ablation volumes in the acute, subacute, and chronic groups of IRECT were respectively 80% (1 day), 81% (3 days), and 124% (7 days) larger than in the respective IRE groups. Moreover, in an intraindividual comparison, in each animal, ablation volumes of the IRECT were always larger than of the IRE. Statistical significance was reached based on CT 1 day and 3 days after the intervention. Ablations calculated on histopathological analysis were systematically larger than based on CT with a mean difference of 1.00 ml for volumes and 0.32 cm for diameters.

Discussion

The percutaneous CT-guided placement of our expandable applicator prototype was feasible without any puncture-related complications even despite the relatively thick diameter. In addition, the reliable deployment of the expandable electrodes, resulting in the intended applicator geometry, was possible in every animal. Therefore, the presented single-needle applicator concept may be suitable to overcome the placement of multiple electrodes, which leads to time-consuming interventions and represents currently a major technical challenge of IRE. So far, only one working expandable prototype in the spectrum of electroporation was described. In 2011, Mahmood et al designed an expandable applicator for the application of ECT in the brain [14] which was subsequently tested in tumor-bearing mice [15]. In this experiment, the applicator performed a pure ECT (280 V/cm); the chemotherapeutic agent was injected intracranially and the different electrodes were powered sequentially, constituting a significant difference compared with our system.

Moreover, standard IRE is associated with a high incidence of needle track seeding, reaching up to 26% of treated patients in a case series including 29 patients with 43 liver tumors [16]. The placement of multiple electrodes in and around the tumor may be associated with the risk of seeding of tumor cells and the expandable design of the applicator could represent a winning strategy to avoid this complication.

Until now, only Tarantino et al published their results on percutaneous ECT in the liver. In their work published in 2017, the authors present a case series of 6 patients with HCC with portal vein tumor thrombosis which was treated with ECT applied using long needle-shaped applicators. They observed no local recurrence in the follow-up with a median of 14 months [4]. The same group reported in 2018 on the first treatment of hilar cholangiocellular carcinoma with ECT. A total of 5 patients were treated and 3/5 patients showed complete response 4 weeks after the intervention [17].

In our experiments, the interstitial administration of chemotherapeutic agent was associated with larger ablation volumes compared with the ablation volumes of IRE only. According to the imaging and the pathological analyses, the regularity of the shape of the ablation volumes of IRE clearly retraces the core of the area of irreversible electroporation according to the computer-simulated analysis. The zone of necrotic tissue corresponds to the area surrounding the central electrode with the expansion of necrosis in direction of the four expandable electrodes. The ablations of the IRECT group were larger and more irregularly shaped. This may be due to the increased cellular uptake of doxorubicin in the periphery of ablation volumes, which is reversibly electroporated and consequently presents a higher permeability of cell membranes. The periphery of IRE ablation zones, where cells are in a reversible state of electroporation because of a decrement in field strength, makes them an ideal candidate for ECT. Up to now, this topic was successfully investigated in vitro by Neal et al in a glioma model [18] and its use in humans firstly described by Klein at al in 2017, who reported successful results of IRECT for the treatment of two lymph node metastases from gastric cancer [19].

In one case, a swine deceased during the intervention due to ventricular fibrillation. It is well established that during the clinical application of IRE, ECG synchronization is mandatory to avoid the risk of arrhythmia [20]. However, due to the experimental nature of our pulse generator, this was not yet possible and represents an engineering challenge for we are currently working on.

A limitation of the present study is the absence of a tumor model. However, stable tumor models are possible only in smaller animals and the dimension of the applicator did not allow its application in smaller animals. Moreover, the size of the experimental group is limited to ten animals due to the animal experiment regulatory board allowance. Statistical significance was reached just based on CT data 1 day and 3 days after the intervention, which are the largest samples in our casuistry: CT 1 day after the intervention was performed on 9 animals and 3 days after the intervention on 6 animals; all the other follow-up groups consists of 3 animals, a too small sample size to reach statistically significant results. A potential limitation of the study is the choice of doxorubicin as chemotherapeutic agent, whereas bleomycin or cisplatin is the most commonly used drug for ECT. Anyway, our clinical experience with hepatocellular carcinoma together with the molecular polarity of doxorubicin [21] led our choice towards this drug. No pure chemoablation with doxorubicin was

performed. Due to the dimensions of the liver and to the anatomy of swines, it was not possible to locate three ablation areas that were separated in a way that interactions between groups can be excluded. Further researches on the effects of different volumes, formulations, and concentrations of drugs on the ablation volumes, as performed with combination of radiofrequency and saline infusion [22] or liposomal doxorubicin [23], are needed to optimize this technique.

In conclusion, the use of the newly developed applicator provides significant advantages compared with the current IRE system; in particular, working with an expandable geometry applicator could permit a faster and safer placement and, in the future, may overcome the limitations of current IRE. Moreover, the interstitial injection of chemotherapeutic agent results in significantly larger ablation volumes compared with IRE alone, rendering the investigation of how to exploit the penumbra of IRE ablations a promising topic for further research.

Funding This work was funded by the German Research Foundation (DFG) under project number 116510359.

Compliance with ethical standards

Guarantor The scientific guarantor of this publication is Prof. Philipp Bruners.

Conflict of interest The authors of this manuscript declare no relationships with any companies whose products or services may be related to the subject matter of the article.

Statistics and biometry One of the authors has significant statistical expertise; moreover, no complex statistical methods were necessary for this paper.

Informed consent Approval from the institutional animal care committee was obtained.

Ethical approval Institutional Review Board approval was not required because it was not necessary after the approval from the institutional animal care committee.

Methodology
- prospective
- experimental
- performed at one institution

References

1. Rubinsky B (2007) Irreversible electroporation in medicine. Technol Cancer Res Treat 6:255–260
2. Miklavčič D, Mali B, Kos B, Heller R, Serša G (2014) Electrochemotherapy: from the drawing board into medical practice. Biomed Eng Online 13. https://doi.org/10.1186/1475-925X-13-29
3. Gehl J, Sersa G, Matthiessen LW et al (2018) Updated standard operating procedures for electrochemotherapy of cutaneous tumours and skin metastases. Acta Oncol 25:874–882
4. Tarantino L, Busto G, Nasto A et al (2017) Percutaneous electrochemotherapy in the treatment of portal vein tumor thrombosis at hepatic hilum in patients with hepatocellular carcinoma in cirrhosis: a feasibility study. World J Gastroenterol 23:906–918
5. Wichtowski M, Murawa D, Kulcenty K, Zaleska K (2017) Electrochemotherapy in breast cancer - discussion of the method and literature review. Breast Care (Basel) 12:409–414
6. Plaschke CC, Bertino G, McCaul JA et al (2017) European Research on electrochemotherapy in Head and Neck Cancer (EURECA) project: results from the treatment of mucosal cancers. Eur J Cancer 87:172–181
7. Bertaccini C, Margotti PM, Bergamini E, Lodi A, Ronchetti M, Cadossi R (2007) Design of an irreversible electroporation system for clinical use. Technol Cancer Res Treat 6:313–320
8. Nault JC, Sutter O, Nahon P, Ganne-Carrié N, Séror O (2017) Percutaneous treatment of hepatocellular carcinoma: state of the art and innovations. J Hepatol 68:783–797
9. Venkat S, Hosein PJ, Narayanan G (2015) Percutaneous approach to irreversible electroporation of the pancreas: Miami protocol. Tech Vasc Interv Radiol 18:153–158
10. Vroomena LGPH, Petrea EN, Cornelis FH, Solomona SB, Srimathveeravalli G (2017) Irreversible electroporation and thermal ablation of tumors in the liver, lung, kidney and bone: what are the differences? Diagn Interv Imaging 98:609–617
11. Marty M, Sersa G, Garbay JR et al (2006) Electrochemotherapy – an easy, highly effective and safe treatment of cutaneous and subcutaneous metastases: results of ESOPE (European Standard Operating Procedures of Electrochemotherapy) study. EJC Suppl 4:3–13
12. Ritter A, Bruners P, Isfort P et al (2018) Electroporation of the liver: more than 2 concurrently active, curved electrodes allow new concepts for irreversible electroporation and electrochemotherapy. Technol Cancer Res Treat 1(17). https://doi.org/10.1177/1533033818809994
13. Ritter A (2017) Strategies and electrode design for the patient-customized application of electroporation in tumor therapy https://doi.org/10.18154/RWTH-2017-08074
14. Mahmood F, Gehl J (2011) Optimizing clinical performance and geometrical robustness of a new electrode device for intracranial tumor electroporation. Bioelectrochemistry 81. https://doi.org/10.1016/j.bioelechem.2010.12.002
15. Agerholm-Larsen B, Iversen HK, Ibsen P et al (2011) Preclinical validation of electrochemotherapy as an effective treatment for brain tumors. Cancer Res 71:3753–3762
16. Distelmaier M, Barabasch A, Heil P et al (2017) Midterm safety and efficacy of irreversible electroporation of malignant liver tumors located close to major portal or hepatic veins. Radiology 285:1023–1031
17. Tarantino L, Busto G, Nasto A et al (2018) Electrochemotherapy of cholangiocellular carcinoma at hepatic hilum: a feasibility study. Eur J Surg Oncol 44:1603–1609
18. Neal RE 2nd, Rossmeisl JH Jr, D'Alfonso V et al (2014) In vitro and numerical support for combinatorial irreversible electroporation and electrochemotherapy glioma treatment. Ann Biomed Eng 42:375–487
19. Klein N, Zapf S, Gunther E, Stehling M (2017) Treatment of lymph node metastases from gastric cancer with a combination of irreversible electroporation and electrochemotherapy: a case report. Clin Case Rep 5:1389–1394
20. Deodhar A, Dickfeld T, Single GW et al (2011) Irreversible electroporation near the heart: ventricular arrhythmias can be prevented

with ECG synchronization. AJR Am J Roentgenol 196. https://doi.org/10.2214/AJR.10.4490

21. Tewes F, Munnier E, Antoon B et al (2007) Comparative study of doxorubicin-loaded poly(lactide-co-glycolide) nanoparticles prepared by single and double emulsion methods. Eur J Pharm Biopharm 66:488–492
22. Miao Y, Ni Y, Mulier S et al (1997) Ex vivo experiment on radiofrequency liver ablation with saline infusion through a screw-tip cannulated electrode. J Surg Res 71(1):19–24
23. Ahmed M, Lukyanov AN, Torchilin V, Tournier H, Schneider AN, Goldberg SN (2005) Combined radiofrequency ablation and adjuvant liposomal chemotherapy: effect of chemotherapeutic agent, nanoparticle size, and circulation time. J Vasc Interv Radiol 16(10):1365–1371